

# Mass function of haloes: scale invariant models

J. S. Bagla, Nishikanta Khandai and Girish Kulkarni

*Harish-Chandra Research Institute, Chhatmag Road, Jhansi,  
Allahabad 211019, INDIA  
E-Mail: jasjeet, nishi, girish@hri.res.in*

2 November 2018

## ABSTRACT

Press-Schechter theory gives a simple, approximate functional form of the mass function of dark matter haloes. Sheth and Tormen (ST) refined this mass function to give an improved analytical fit to results of  $N$ -body simulations. These forms of the halo mass function are universal (independent of cosmology and power spectrum) when scaled in suitable variables. Using large suites of LCDM  $N$ -body simulations, studies in the last few years have shown that this universality is only approximate. We explore whether some of the deviations from universality can be attributed to the power spectrum by computing the mass function in  $N$ -body simulations of various scale-free models in an Einstein-de Sitter cosmology. This choice of cosmology does not introduce any scale into the problem. These models have the advantage of being self-similar, hence stringent checks can be imposed while running these simulations. This set of numerical experiments is designed to isolate any power spectrum dependent departures from universality of mass functions. We show explicitly that the best fit ST parameters have a clear dependence on power spectrum. Our results also indicate that an improved analytical theory with more parameters is required in order to provide better fits to the mass function.

**Key words:** gravitation, methods: N-Body simulations, cosmology: large scale structure of the universe

## 1 INTRODUCTION

The halo mass function describes number density of dark matter haloes of a given mass in a given cosmology, and is an essential input for a diverse set of tools used for making theoretical predictions. The halo model of large scale structure, for example, is based on the theory of mass functions (Cooray & Sheth 2002). Accurate knowledge of the mass function is important for several cosmological applications, including semi-analytic theories of galaxy formation (White & Frenk 1991); constraints on cosmological parameters using galaxy cluster abundance (Majumdar & Mohr 2003), gravitational lensing (Bartelmann et al. 1998) and constraints on non-Gaussianity in the primordial power spectrum (Bartolo, Matarrese, & Riotto 2005) of matter perturbation.

It is possible to develop the theory of mass functions in a manner that makes no reference to the details of the cosmological model or the power spectrum of fluctuations. That is, we expect the mass function to take a universal form, when scaled appropriately. Simple theoretical arguments have been used to obtain this universal functional form of the mass function (Press & Schechter 1974; Bond et al. 1991; Sheth, Mo, & Tormen 2001). Bond et al. (1991) and Sheth, Mo, & Tormen (2001) used the excursion set theory to derive the mass function. Much work has also been done to determine the extent to which this form is consistent with results from  $N$ -body simulations (Jenkins et al. 2001; White 2002; Reed et al. 2003; Warren et al. 2006; Reed et al. 2007; Lukić et al. 2007;

Cohn & White 2008; Tinker et al. 2008) with the conclusion that the agreement is fairly good. Recent comparisons with very large  $N$ -Body simulations also provide hints that the form of the mass function is not universal.

The Press-Schechter mass function (Press & Schechter 1974) is based on the spherical collapse model (Gunn & Gott 1972) and the ansatz that the mass in collapsed objects is related to the volume with density above a certain threshold. The shape of the mass function agrees with numerical results qualitatively: at a quantitative level there are deviations at the low mass and the high mass ends (Efstathiou et al. 1988; Jenkins et al. 2001). Improvements to the Press-Schechter mass function have been made to overcome this limitation. In particular, the Sheth-Tormen mass function is based on the more realistic ellipsoidal collapse model (Sheth & Tormen 1999; Sheth, Mo, & Tormen 2001) and it fits numerical results better. These mass functions relate the abundance of haloes to the initial density field in a universal manner, independent of cosmology and power spectrum. Many fitting functions with three or four fitting parameters have been proposed. These are based on results of simulations of the LCDM model (Jenkins et al. 2001; Reed et al. 2003; Warren et al. 2006).

In the last few years, large  $N$ -Body simulations of the LCDM model have demonstrated that the mass function is not universal (White 2002), and epoch dependent fitting functions have been given for this model (Reed et al. 2007; Tinker et al. 2008). The

results of Lacey & Cole (1994) also show a small dependence of the mass function on the power spectrum but given the size of simulations these deviations are small. These studies show non-universality by noting variations in the form of mass function with redshift or cosmology in successively larger simulations that explore a large range in mass. Much of the numerical work in this area during the last decade has focused on the LCDM model, it being the model favored by observations.

It is expected that this non-universality is a result of variation of mass function parameters either with cosmology or with the power spectrum or both. Cosmology dependence is introduced by the variation in the threshold density for collapse (Barrow & Saich 1993). The CDM class of models have a power spectrum of density fluctuations with a gradually varying slope or the spectral index,  $n(k)$ , which decreases with decreasing scale (increasing wavenumber  $k$ ). As perturbations at smaller scales collapse earlier, the effective index of the power spectrum is small at early times and increases towards late times. The threshold overdensity for collapse also changes as the cosmological constant becomes more important at late times. Thus the variation in mass function may be due to the shape of the power spectrum, or cosmology, or both. This makes the published results difficult to interpret in terms of a theoretical model. It is then hard to discern any trends in non-universality that will potentially provide a physical understanding. Given the number of applications of the theory of mass function like computation of merger rates, halo formation rates, etc., it is essential to develop a clear understanding of the origin of non-universality. The only other option is to work with fitting functions for each of these quantities derived from N-Body simulations.

The problem of an unclear origin of deviations of universality can be partially addressed by studying a wider variety of models in the CDM class of models. This approach has been taken by, for example, Neistein, Maccio, & Dekel (2009) in the context of universality in halo mergers. The effect of perturbations at larger scales in terms of the tidal field, which is relevant for ellipsoidal collapse, also changes with time due to the variation in the slope of the power spectrum with scale. Given that the tidal field is generated by larger scales, it is not very clear whether a prescription based on the local index of the power spectrum alone can provide a detailed explanation for the mass function. Since the CDM spectra lack the simplicity of the scale-free spectra, we approach this problem differently. We specifically look for departures from non-universality in the mass function for scale-free power spectrum of initial fluctuations with an Einstein-de Sitter background to check if the non-universal description can be attributed to a spectrum dependence. Our choice of cosmology does not introduce any scale in the problem and the threshold overdensity does not vary with time in any non-trivial manner. Thus we can isolate the non-universality of mass functions arising from the slope of the power spectrum. We provide spectrum dependent fits for the parameters in the Sheth-Tormen mass function, and show that this allows us to fit simulation data much better.

We start with a discussion of the basic framework of mass functions in §2, where we also set up the notation. Our numerical simulations are described in §3. We present our analysis of the data in §4 along with the results. A discussion of their implications appears in §5 and we summarize our conclusions in §6.

**Table 1.** Details of  $N$ -body simulations used in this work.

$n$	$N_{\text{box}}$	$N_{\text{part}}$	$r_{\text{nl}}^i$	$r_{\text{nl}}^f$	$r_{\text{nl}}^{\text{max}}$	$z_i$
-2.5	$512^3$	$512^3$	0.2	1.0	0.1	36.21
-2.2	$512^3$	$512^3$	0.5	2.0	2.0	51.23
-2.0	$512^3$	$512^3$	1.0	4.5	4.2	62.80
-1.8	$512^3$	$512^3$	2.5	9.0	8.5	78.82
-1.5	$400^3$	$400^3$	2.5	12.0	10.0	103.38
-1.0	$400^3$	$400^3$	2.5	10.0	22.2	171.52
-0.5	$256^3$	$256^3$	2.5	12.0	18.2	291.53
+0.0	$256^3$	$256^3$	2.5	12.0	21.2	470.81

## 2 THE MASS FUNCTION

The mass function is described by the following function in the Press-Schechter formalism:

$$f(\nu) = \sqrt{\frac{2}{\pi}} \nu \exp(-\nu^2/2) \quad (1)$$

where  $\nu = \delta_c / (\sigma(m)D_+(z))$ . Here  $\delta_c$  is the threshold overdensity for a spherically symmetric perturbation, above which it collapses and forms a virialised halo. It has only a weak dependence on cosmology and its value is 1.69 for  $\Omega_0 = 1$  (Gunn & Gott 1972; Peebles 1980). Fitting functions that describe the dependence of  $\delta_c$  on cosmology are available in the literature (Barrow & Saich 1993; Eke, Cole, & Frenk 1996; Navarro, Frenk, & White 1996; Nakamura & Suto 1997; Bryan & Norman 1998; Henry 2000). We take the value of 1.686 throughout our analysis as we are working with the Einstein-de Sitter cosmology.

The *rms* fluctuations of the linearly evolved density field at present is denoted by  $\sigma(m)$ , smoothed with a spherical top hat filter enclosing mass  $m$  and is calculated by convolving the linear density power spectrum  $P(k)$ , extrapolated to the current epoch, with the filter  $W(k, m)$ :

$$\sigma^2(m) = \int_0^\infty \frac{dk}{k} \frac{k^3 P(k)}{2\pi^2} W^2(k, m). \quad (2)$$

Lastly,  $D_+(z)$  is the growth function (Heath 1977). All mass is contained in haloes in this formalism, this provides the normalization:

$$\int_0^\infty \frac{1}{\nu} f(\nu) d\nu = 1 \quad (3)$$

This mass function is related to the number of haloes of a given mass per unit comoving volume by

$$\frac{dn}{d \ln m} = \frac{\bar{\rho}}{m} \frac{d \ln \sigma^{-1}}{d \ln m} f(\nu). \quad (4)$$

The dependence on cosmology and power spectrum is absorbed in  $\nu$ , and the theory of mass functions can be developed without reference to the detailed dependence of  $\nu$  on the power spectrum or cosmology, so we expect the form of Equation (1) to be universal.

The Sheth-Tormen mass function is a modification to the Press-Schechter model and is based on ellipsoidal collapse instead of spherical collapse. It has been shown to reproduce simulation results better.

$$f(\nu) = A \sqrt{\frac{2q}{\pi}} [1 + (q\nu^2)^{-p}] \nu \exp(-q\nu^2/2). \quad (5)$$

Clearly, this is also a universal form.

### 3 NUMERICAL SIMULATIONS

We run a suite of models with a power law power spectrum ( $P(k) = Ak^n$ ) of initial fluctuations, in the range  $-2.5 \geq n \geq 0.0$ . We use the Einstein-de Sitter cosmological background where the growing mode of perturbations  $D_+(t)$  is the same as the scale factor  $a(t)$ . We used the TreePM code (Khandai & Bagla 2009) for these simulations. The TreePM (Bagla 2002; Bagla & Ray 2003) is a hybrid N-Body method which improves the accuracy and performance of the Barnes-Hut (BH) Tree method (Barnes & Hut 1986) by combining it with the PM method (Miller 1983; Klypin & Shandarin 1983; Bouchet, Adam, & Pellat 1985; Bouchet & Kandrup 1985; Hockney & Eastwood 1988; Bagla & Padmanabhan 1997; Merz, Pen, & Trac 2005). The TreePM method explicitly breaks the potential into a short-range and a long-range component at a scale  $r_s$ : the PM method is used to calculate long-range force and the short-range force is computed using the BH Tree method. Use of the BH Tree for short-range force calculation enhances the force resolution as compared to the PM method.

The mean interparticle separation between particles in the simulations used here is  $l_{\text{mean}} = 1.0$  in units of the grid-size used for the PM part of the force calculation. In our notation this is also cube root of the ratio of simulation volume  $N_{\text{box}}^3$  to the total number of particles  $N_{\text{part}}$ .

Power law models do not have any intrinsic scale apart from the scale of non-linearity introduced by gravity. We can therefore identify an epoch in terms of the scale of non-linearity  $r_{\text{nl}}$ . This is defined as the scale for which the linearly extrapolated value of the mass variance at a given epoch  $\sigma_L(a, r_{\text{nl}})$  is unity. All simulations are normalized such that  $\sigma^2(a = 1.0, r_{\text{nl}} = 8.0) = 1.0$ . The softening length in grid units is  $\epsilon = 0.03$  in all runs.

Simulations introduce an inner and an outer scale in the problem and in most cases we work with simulation results where  $L_{\text{box}} \gg r_{\text{nl}} \geq L_{\text{grid}}$ , where  $L_{\text{grid}}$ , the size of a grid cell is the inner scale in the problem.  $L_{\text{box}}$  is the size of the simulation and represents the outer scale.

Finite volume effects can lead to significant errors in N-Body simulations since modes greater than the size of the box are ignored while generating initial conditions and during evolution (Bagla & Ray 2005; Bagla & Prasad 2006; Power & Knebe 2006; Bagla, Prasad, & Khandai 2009). The errors in the mass variance and hence most descriptors of clustering can become arbitrarily large as the index of the power spectrum  $n$  approaches  $-3.0$ . The prescription provided by Bagla & Prasad (2006) and Bagla, Prasad, & Khandai (2009) can be used to find the regime where the results of a simulation are reliable at a given level of tolerance. We require that the error in  $\sigma^2$  be less than 3% at the scale of non-linearity. This requirement severely restricts the level of non-linearity that can be probed in simulations with indices  $n = -2.5, -2.2$  and  $-2.0$  amongst the set of models we use here. We will use these simulations mainly to illustrate the severity of finite box size effects and compare the mass function obtained in the simulations with our expectations, but we do not use these simulations for an explicit determination of the mass function. In Table (1) we list the power law models simulated for the present study. We list the index of the power spectrum  $n$  (column 1), size of the simulation box  $N_{\text{box}}$  (column 2), number of particles  $N_{\text{part}}$  (column 3), the scale of non-linearity at the earliest epoch used in this study (column 4), and, the maximum scale of non-linearity,  $r_{\text{nl}}^{\text{max}}$  (column 6) given our tolerance level of 3% error in the mass variance at this scale. For some models with very negative indices we have run the simu-

lations beyond this epoch, as can be seen in column 5 where we list the actual scale of non-linearity for the last epoch.

In the next section we describe a procedure to put an upper limit on the high mass bins since in these haloes counts are reduced due to finite boxsize considerations, especially at late times. The counts of haloes in low mass bins are relatively unaffected by finite box considerations. We therefore limit errors in the mass function by running the simulation up to  $r_{\text{nl}}^{\text{max}}$ . Column 7 lists the starting redshift of the simulations for every model.

Models with a large slope of the power spectrum have more power at small scales and the relative amplitude of fluctuations at small scales is large. Care is required for running simulations of these models as small scales become non-linear at early times the  $r_{\text{nl}}$  grows very slowly with the scale factor. A very large number of time steps are required in order to evolve the system to epochs with a large  $r_{\text{nl}}$ . We require that the evolution of the two point correlation function  $\xi$  (Peebles 1980) be strictly self-similar in the range of epochs where we use the simulation data. This allows us to verify the correctness of evolution.

### 4 ANALYSIS AND RESULTS

We use the Friends-of-Friends (FOF) (Davis et al. 1985) algorithm with a linking length  $l = 0.2$  to identify haloes and construct a halo catalog. In order to avoid spurious identification of haloes and also discreteness noise, we do not use haloes with a small number of particles — only haloes with more than 60 particles are used in our analysis.

Given the halo catalog one can compute the mass function by first binning the haloes in mass bins. We constructed logarithmic bins in mass with size  $\Delta \log m = 0.2$ . Given the halo count per logarithmic mass bin  $dn/d \log m$  and using the fact that  $\bar{\rho} = 1$ , we write Equation 4

$$f(\nu) = \frac{6}{n+3} \frac{m}{\bar{\rho}} \frac{dn}{d \ln m} \quad (6)$$

with  $\nu = \delta_c/a \sigma(m)$ . For a power law power spectrum, we have

$$\sigma(m) = \left( \frac{m}{m_{\text{nl}}} \right)^{-(n+3)/6} \quad (7)$$

where  $m = 4\pi r^3/3$ , and we take  $r_{\text{nl}}(z = 0) \equiv 8.0$ . Note that Equation (7) tells us that it is much easier to probe the small  $\nu$  end of the mass function with larger indices. The scale of non-linearity evolves as  $r_{\text{nl}} \propto D_+^{2/(n+3)} = a^{2/(n+3)}$ , where the second equality follows for the Einstein-de Sitter universe.

We choose to fit the Sheth-Tormen mass function of Equation (5) to our data by the method of  $\chi^2$  minimization. The correspondence with the mass function for ellipsoidal collapse makes the Sheth-Tormen mass function physically motivated. The usefulness of this approach is that the best fit values can potentially be used to compute merger rates, etc. This however may not be the best choice of the functional form of the mass function and we comment on it in the following discussion. The ST mass function has two free parameters, which we denote by  $p$  and  $q$ . The condition that all mass must be in haloes provides normalization for this function (Equation (4)). This gives

$$A = 1 + \frac{2^{-p} \Gamma(0.5 - p)}{\sqrt{\pi}} \quad (8)$$

as a function of  $p$  (Cooray & Sheth 2002).

We assume Poisson errors for counts of haloes in a mass bin.

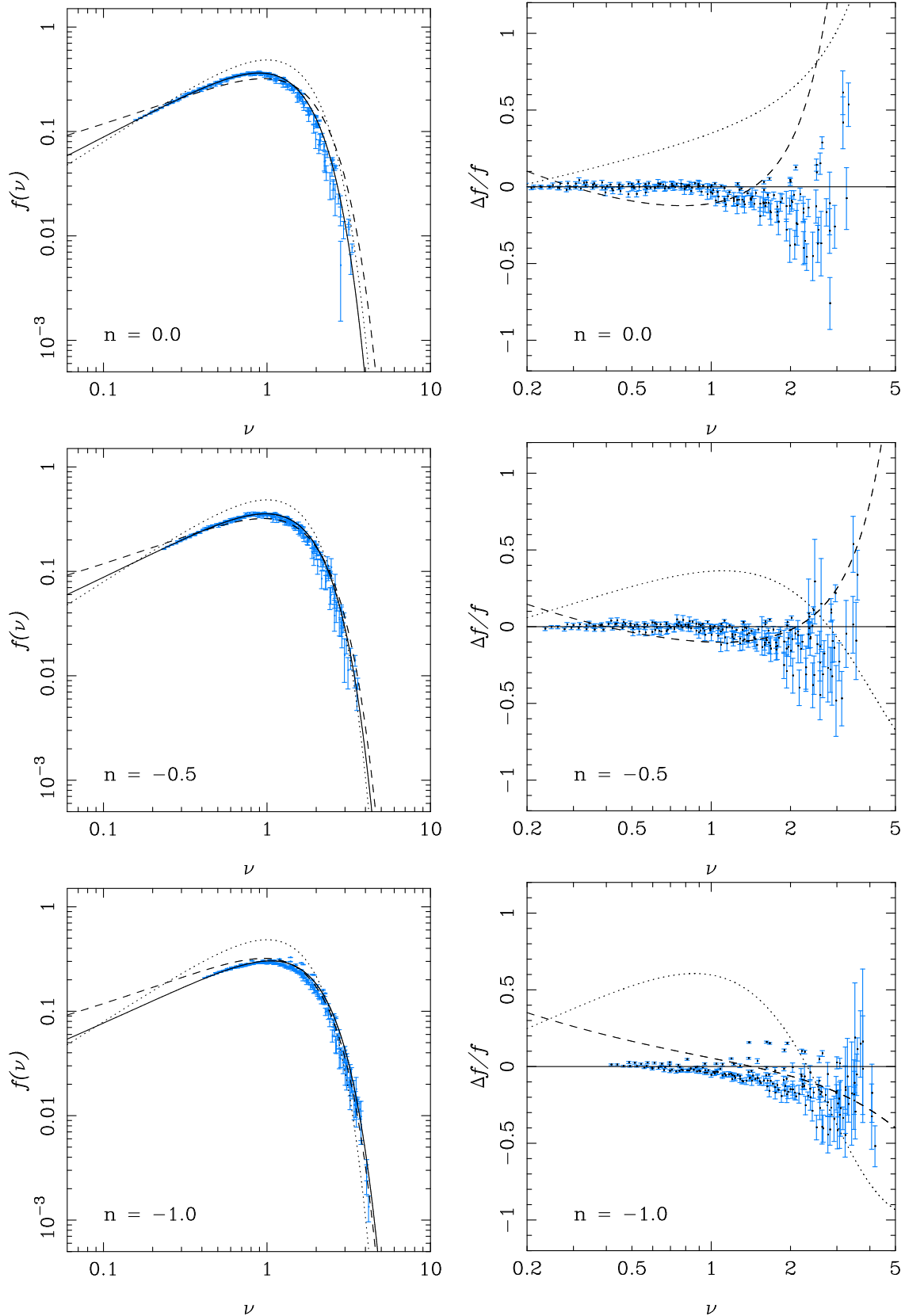


**Figure 1.** Mass functions from our simulations (left column) and their residuals after fitting a Sheth-Tormen form (right column). Rows 1, 2 and 3 are for indices  $n = 0.0, -0.5, -1.0$ . Solid black line is our best fit Sheth-Tormen curve. Dashed line and dotted line show the standard Sheth-Tormen and Press-Schechter curves respectively.

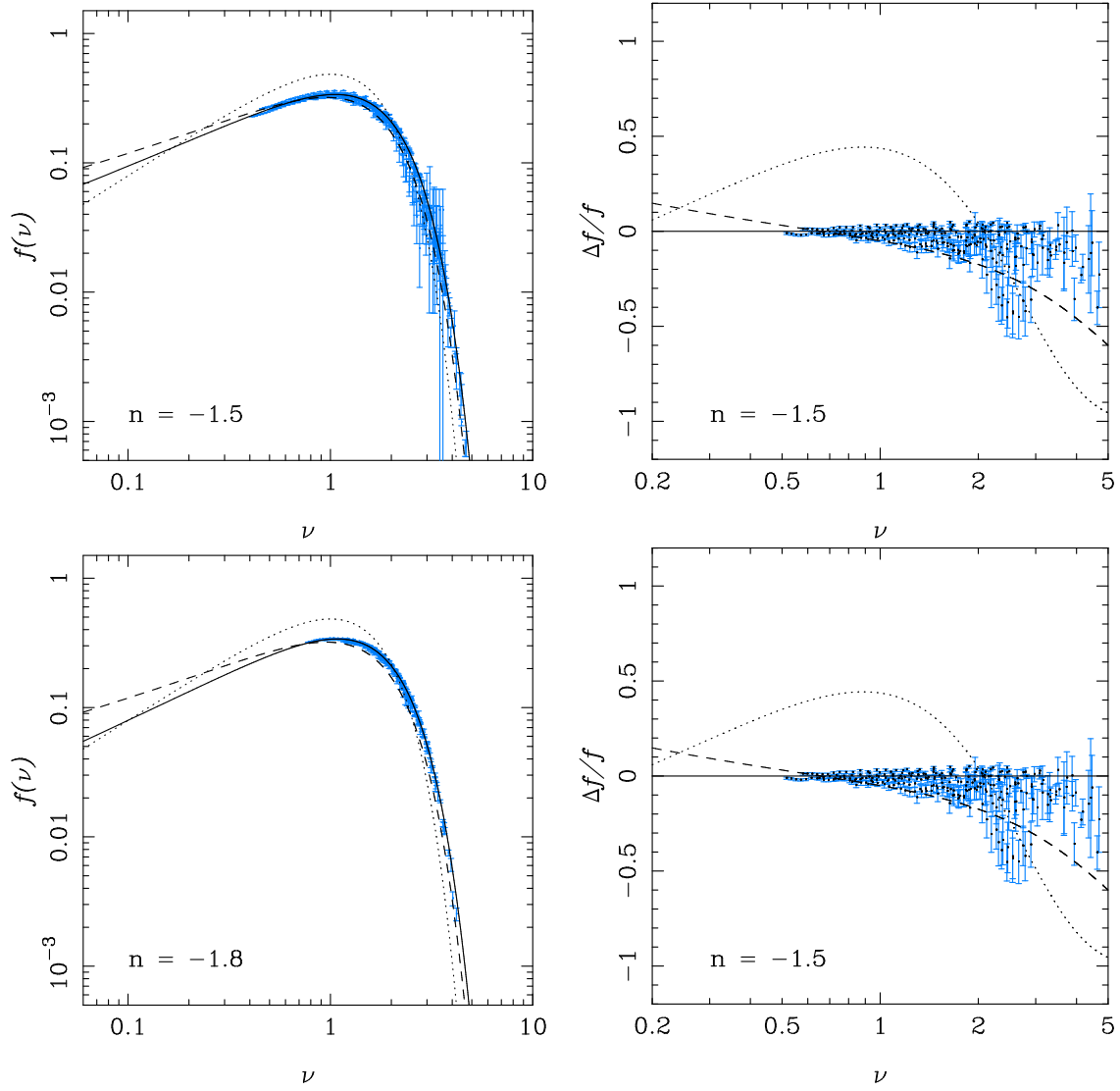


Figure 2. Same as Figure (1) for indices  $n = 1.5$  (top), and  $-1.8$  (bottom).

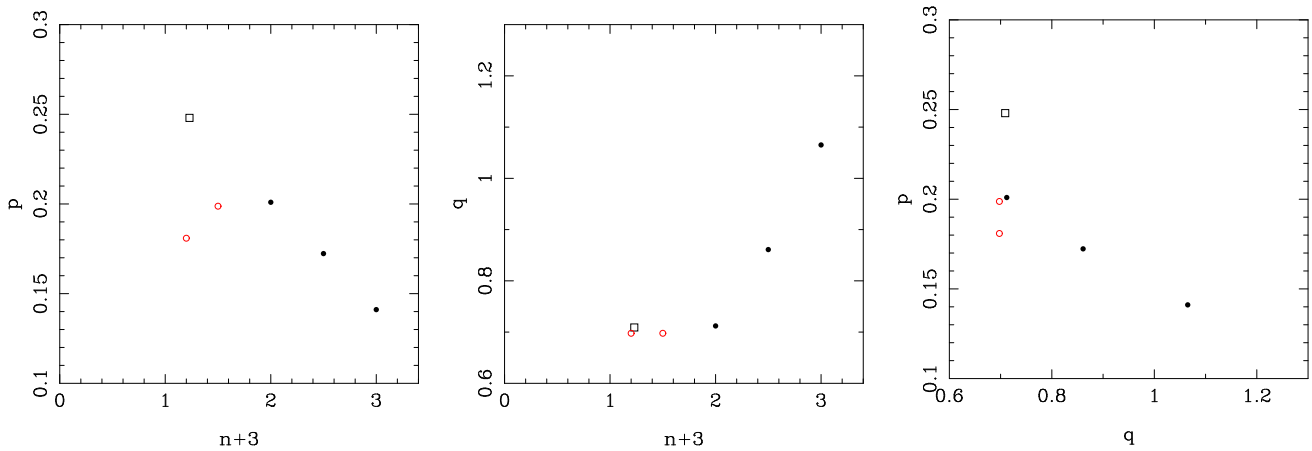


Figure 3. Relation between Sheth-Tormen parameters and the index  $n$  of the power law power spectrum. Red circles denote data with smaller range in  $\nu$ . The square denotes the value of Manera, Sheth, & Scoccimarro (2009). See text for details.

**Table 2.** Best fit parameters of Sheth-Tormen mass function

$n$	$p$	$q$	$\chi_{\text{red}}^2$	$p^{\text{new}}$	$q^{\text{new}}$	$\chi_{\text{red}}^{2(\text{new})}$
0.0	0.141	1.065	4.933	—	—	—
-0.5	0.172	0.861	3.24	—	—	—
-1.0	0.201	0.712	31.31	—	—	—
-1.5	0.199	0.698	4.87	0.232	0.684	5.64
-1.8	0.181	0.698	4.760	0.250	0.677	6.23
-2.0	—	—	—	0.262	0.677	3.94
-2.2	—	—	—	0.274	0.698	4.56

As discussed before, the effect of a finite volume simulation volume suppresses the count of haloes in the large mass end. One can either correct it (Reed et al. 2007, 2009) or remove these points from the  $\chi^2$  analysis. Correcting for these points is a tricky issue since it assumes a priori knowledge of the mass function, the quantity which is being constructed. One can however follow an iterative procedure by first starting out with the standard ST mass function or the Press-Schechter mass function, then use it to correct the counts at the large mass end of the mass function and then do the  $\chi^2$  analysis to compute a better ST mass function and repeat the exercise all over again until one obtains a reasonable convergence in the fit. As we shall see, the dispersion and the goodness of fit does not warrant this approach and in this paper we choose to remove points affected by more than 10% in counts (as compared to expected PS counts) due to box size effects.

We begin by fitting the ST mass function to the indices  $n = 0.0, -0.5, -1.0, -1.5$  and  $-1.8$ . The raw mass function, i.e., data points, and the best fit ST curve is plotted in the left column of Figures (1) and (2). The right hand column shows the residuals with respect to the best fit mass function. We also show the PS and the standard ST mass functions in each panel. Table (2) shows the best fit values of  $p$  and  $q$  and the reduced  $\chi_{\text{red}}^2$ .

## 5 DISCUSSION

At the outset a visual inspection of Figure (1) shows a clear trend in the shape of the mass function with index  $n$  of the power spectrum. We also see that the evolution is self-similar across different epochs for all indices. This is as expected for power law models in Einstein-de Sitter background.

In Figures (1) and (2) we find that for the more negative indices  $n = -1.8, -1.5, -1.0$  we have a smaller dynamic range in  $\nu$  as compared to  $n = -0.5, 0.0$ . This is expected given that we have not evolved simulations with these indices over large range of epochs due to finite boxsize considerations. Since the slope of  $f(\nu)$  at the small  $\nu$  end is related to  $p$  — it is  $f(\nu) \propto \nu^{1-2p}$  as  $\nu \rightarrow 0$  — one cannot trust these results as much as the results with  $n = -0.5$  and  $0.0$  which probe  $f(\nu)$  out to much smaller values in  $\nu$ . The best fit values of  $(p, q)$  and  $\chi_{\text{red}}^2$  are shown in columns 2, 3 and 4 of Table 2 for every model (column 1). Surprisingly  $\chi_{\text{red}}^2$  is relatively low for all indices as compared to the index  $n = -1.0$ . Part of this is due to several outliers for the  $n = -1.0$  spectrum which have more than  $10\sigma$  deviations. Removing these points we find that  $\chi_{\text{red}}^2 = 11.3$  from the original value of  $\chi_{\text{red}}^2 = 31.6$ . The corresponding values of  $(p, q)$  changes to  $(p, q) = (0.22, 0.73)$  from  $(p, q) = (0.20, 0.71)$ . In Figure (3) we also add the best fit value of  $p$  and  $q$  from the recent work of Manera, Sheth, & Scocci-

marro (2009), which used 49 realizations of an LCDM simulation with  $640^3$  particles in a box of side  $L_{\text{box}} = 1280h^{-1}\text{Mpc}$ . We identify the effective index at  $z = 0$ , by computing

$$\left. \frac{d \log \sigma(m)}{d \log m} \right|_{\sigma=1} = -\frac{(n_{\text{eff}} + 3)}{6} \quad (9)$$

Next we look at the dependence of the two ST parameters  $(p, q)$  on the index of the spectrum  $n$  and also their inter-dependence. In Figure (3) we find that all the trends seen between  $p, q$  and  $n$  ( $n_{\text{eff}}$  for LCDM) are smooth when one considers the LCDM model and the power law models with indices  $n = 0.0, -0.5, -1.0$ . We find that the relation between  $p$  and  $n$  is approximately

$$p(n) \simeq -0.0605 n + 0.141 \quad (10)$$

The trends in these parameters show deviations when one adds the models  $n = -1.5$  and  $-1.8$ , especially in the values of  $p$ ; deviations in  $q$  are not as drastic. However if we use Equation (10) and fix  $p$  for the indices  $n = -1.5, -1.8$  and redo the  $\chi^2$  analysis to fit  $q$  then the  $\chi^2$  does not change much, thereby corroborating our argument that the values of  $p$  for the models  $n = -1.5, -1.8$  are unreliable due to the small range in  $\nu$ . The new values of  $p^{\text{new}}, q^{\text{new}}, \chi_{\text{red}}^{2(\text{new})}$  are listed in columns 5-7 of Table (2). Figure (4) plots the best fit ST curve using the extrapolated value of  $p$  for the models  $n = -1.5, -1.8, n = -2.0$  and  $-2.2$ . Since we have not probed highly non-linear scales for these models the range of  $\nu$  is even more limited, so much so that a full  $\chi^2$  minimization for  $(p, q)$  is futile. We therefore do not list the best fit values of  $(p, q)$  in Table (2) and proceed to do a similar fitting using Equation (10) for the models  $n = -2.0, -2.2$  and find that  $\chi_{\text{red}}^{2(\text{new})}$  is in the same range as for other models. The values  $p^{\text{new}}, q^{\text{new}}, \chi_{\text{red}}^{2(\text{new})}$  for these models are given in columns 5-7 of Table (2). Again we find that the  $\chi_{\text{red}}^{2(\text{new})}$  is reasonable giving credence to the extrapolation of Equation (10).

However the trend between  $p, q$  and  $n_{\text{eff}}$  is reversed when we compare with the LCDM runs of Manera, Sheth, & Scoccimarro (2009). Here  $p$  decreases and  $q$  increases with increasing redshift (increasing  $n_{\text{eff}}$ ), at  $z = 0.5$ . However at this redshift,  $\Omega_{\Lambda}$  has a dominant role thereby making a simple interpretation difficult. We are carrying out a series of numerical experiments where we simulate power law models in a background cosmology with a cosmological constant to develop further understanding of this issue.

Warren et al. (2006) reported a reduced  $\chi_{\text{red}}^2 \sim 5$  for the Sheth-Tormen mass function with their data. Our values of  $\chi_{\text{red}}^2$  are similar and confirm that the Sheth-Tormen mass function is inadequate in fitting the data in power law models.

The Sheth-Tormen parameters also show a clear dependence on the index of the spectrum. One approach of alleviating this problem would be to better model barrier shape using simple models like the ones we have here. These can then be used to construct and compare with more complicated barriers arising due to different cosmology and a scale dependant index like the CDM class of models. The other approach can be purely phenomenological: one can use results from simpler models like those studied here and understand how further complications in the model, like running index and different cosmologies, affect the shape of the mass function.

Our focus has been on demonstrating that the mass function has a dependence on the slope of the power spectrum. In this study we have not looked at how a change in the definition of the halo—for example, change in the linking length in FOF halo finder or us-

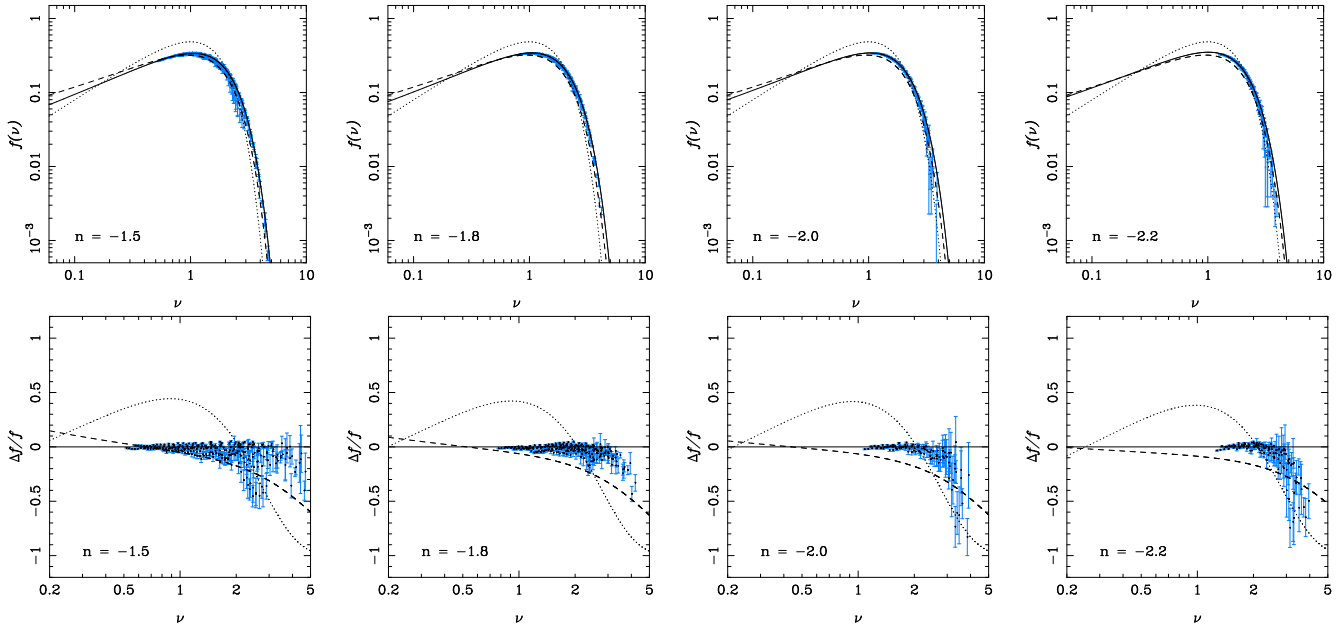


**Figure 4.** Same as Figure (2), except that the solid black line here indicates Sheth-Tormen mass function with parameters obtained by extrapolating  $p(n)$  and  $q(n)$  from  $-1 \leq n \leq 0$  as shown in Figure (3).

ing the SO halo finder instead of FOF (Lacey & Cole 1994; Tinker et al. 2008)—affects the mass function. Indeed one expects that the halo definition changes the amplitude of the mass function (Cohn & White 2008; White 2002; Tinker et al. 2008) but we do not expect it to affect our results in a significant manner. We postpone a study of the dependence of the Sheth-Tormen parameters on halo definition to a later paper.

## 6 CONCLUSIONS

We summarize the conclusions of the present study here.

- We find that the mass function is not universal and has an explicit dependence on the power spectrum.
- The Sheth-Tormen parameters show a systematic trend with index of the power law power spectrum. We also find that there is a correlation between these parameters.
- Evolution of the mass function  $f(\nu)$  in power law models in an Einstein de Sitter background is self-similar, i.e., the functional form does not change with time for a given power law model. We do not expect this in the CDM class of spectra since the effective index,  $n_{\text{eff}}$ , changes with redshift. However, the spectrum dependence of  $p$  and  $q$  is not very strong, and the range over which  $n_{\text{eff}}$  varies is not very large, hence the usual ST parameters are an adequate first approximation. Variation of ST parameters becomes relevant if we require a very precise description of the mass function.
- Our  $\chi^2$  analysis shows that Sheth-Tormen mass function is inadequate and that better modeling of collapse with more parameters is needed.
- Finite box size considerations impose serious limitations on running simulations with large negative indices of the power spectrum. This end of the spectrum probes the mass function of high redshift objects. The way out would be to run orders of magnitude larger simulations for indices with  $n \rightarrow -3$ . This is a challenge

and would be overcome only in the next generation of simulations. An alternative is to use zoom in simulations for such indices.

- For models with  $n \gg -3$ , the rate of growth for  $r_{\text{nl}}$  with time is very slow and as a result a large number of time steps are required for evolving the system. The Adaptive TreePM (Bagla & Khandai 2009) may be useful for running such simulations.

## ACKNOWLEDGMENTS

Computational work for this study was carried out at the cluster computing facility in the Harish-Chandra Research Institute (<http://cluster.hri.res.in/index.html>). This research has made use of NASA's Astrophysics Data System.

## REFERENCES

- Bagla J. S., Padmanabhan T., 1997, *Pramana*, 49, 161  
 Bagla J. S., Prasad J., 2006, *MNRAS*, 370, 993  
 Bagla J. S., Ray S., 2003, *NewA*, 8, 665  
 Bagla J. S., Ray S., 2005, *MNRAS*, 358, 1076  
 Bagla J. S., Prasad J., Khandai N., 2009, *MNRAS*, 395, 918  
 Bagla J. S., 2002, *JApA*, 23, 185  
 Bagla J. S., Khandai N., 2009, *MNRAS*, 396, 2211  
 Barnes J., Hut P., 1986, *Nature*, 324, 446  
 Barrow J. D., Saich P., 1993, *MNRAS*, 262, 717  
 Bartelmann M., Huss A., Colberg J. M., Jenkins A., Pearce F. R., 1998, *A&A*, 330, 1  
 Bartolo N., Matarrese S., Riotto A., 2005, *JCAP*, 10, 10  
 Bond J. R., Cole S., Efstathiou G., Kaiser N., 1991, *ApJ*, 379, 440  
 Bouchet F. R., Kandrup H. E., 1985, *ApJ*, 299, 1  
 Bouchet F. R., Adam J.-C., Pellat R., 1985, *A&A*, 144, 413  
 Bryan G. L., Norman M. L., 1998, *ApJ*, 495, 80  
 Cohn J. D., White M., 2008, *MNRAS*, 385, 2025  
 Cooray A., Sheth R., 2002, *PhR*, 372, 1

## 8 *Bagla, Khandai and Kulkarni*

- Davis M., Efstathiou G., Frenk C. S., White S. D. M., 1985, *ApJ*, 292, 371
- Efstathiou G., Frenk C. S., White S. D. M., Davis M., 1988, *MNRAS*, 235, 715
- Eke V. R., Cole S., Frenk C. S., 1996, *MNRAS*, 282, 263
- Gunn J. E., Gott J. R. I., 1972, *ApJ*, 176, 1
- Heath D. J., 1977, *MNRAS*, 179, 351
- Henry J. P., 2000, *ApJ*, 534, 565
- Hockney R. W., Eastwood J. W., 1988, *Computer Simulation using Particles*, McGraw-Hill
- Jenkins A., Frenk C. S., White S. D. M., Colberg J. M., Cole S., Evrard A. E., Couchman H. M. P., Yoshida N., 2001, *MNRAS*, 321, 372
- Khandai N., Bagla J. S., 2009, *Research in Astronomy and Astrophysics*, 9, 861-873
- Klypin A. A., Shandarin S. F., 1983, *MNRAS*, 204, 891
- Lacey C., Cole S., 1994, *MNRAS*, 271, 676
- Lukić Z., Heitmann K., Habib S., Bashinsky S., Ricker P. M., 2007, *ApJ*, 671, 1160
- Majumdar S., Mohr J. J., 2003, *ApJ*, 585, 603
- Manera M., Sheth R. K., Scoccimarro R., 2009, *arXiv*, 0906.1314
- Merz H., Pen U.-L., Trac H., 2005, *NewA*, 10, 393
- Miller R. H., 1983, *ApJ*, 270, 390
- Nakamura T. T., Suto Y., 1997, *PThPh*, 97, 49
- Navarro J. F., Frenk C. S., White S. D. M., 1996, *ApJ*, 462, 563
- Neistein E., Maccio A. V., Dekel A., 2009, *arXiv*, 0903.1640
- Peebles P. J. E., 1980, *The Large-Scale Structure of the Universe*, Princeton University Press
- Power C., Knebe A., 2006, *MNRAS*, 370, 691
- Press W. H., Schechter P., 1974, *ApJ*, 187, 425
- Reed D., Gardner J., Quinn T., Stadel J., Fardal M., Lake G., Governato F., 2003, *MNRAS*, 346, 565
- Reed D. S., Bower R., Frenk C. S., Jenkins A., Theuns T., 2007, *MNRAS*, 374, 2
- Reed D. S., Bower R., Frenk C. S., Jenkins A., Theuns T., 2009, *MNRAS*, 394, 624
- Sheth R. K., Tormen G., 1999, *MNRAS*, 308, 119
- Sheth R. K., Mo H. J., Tormen G., 2001, *MNRAS*, 323, 1
- Tinker J., Kravtsov A. V., Klypin A., Abazajian K., Warren M., Yepes G., Gottlöber S., Holz D. E., 2008, *ApJ*, 688, 709
- Warren M. S., Abazajian K., Holz D. E., Teodoro L., 2006, *ApJ*, 646, 881
- White S. D. M., Frenk C. S., 1991, *ApJ*, 379, 52
- White M., 2002, *ApJS*, 143, 241